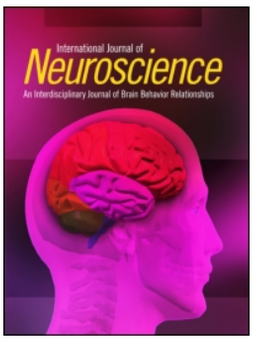

International Journal of Neuroscience

ISSN: (Print) (Online) Journal homepage: https://www.tandfonline.com/loi/ines20

Detection of brain lesion location in MRI images using convolutional neural network and robust PCA

Mohsen Ahmadi, Abbas Sharifi, Mahta Jafarian Fard & Nastaran Soleimani

To cite this article: Mohsen Ahmadi, Abbas Sharifi, Mahta Jafarian Fard & Nastaran Soleimani (2021): Detection of brain lesion location in MRI images using convolutional neural network and robust PCA, International Journal of Neuroscience, DOI: 10.1080/00207454.2021.1883602

To link to this article: https://doi.org/10.1080/00207454.2021.1883602

Published online: 12 Feb 2021.

INTERNATIONAL JOURNAL OF NEUROSCIENCE
https://doi.org/10.1080/00207454.2021.1883602

Taylor & Francis
Taylor & Francis Group

ORIGINAL ARTICLE

Detection of brain lesion location in MRI images using convolutional neural network and robust PCA

Mohsen Ahmadi[a], Abbas Sharifi[b], Mahta Jafarian Fard[c] and Nastaran Soleimani[d]

[a]Department of Industrial Engineering, Urmia University of Technology, Urmia, Iran; [b]Department of Mechanical Engineering, Urmia University of Technology, Urmia, Iran; [c]Department of Electrical Engineering, Islamic Azad University Science and Research, Razavi Khorasan, Iran; [d]Department of Electronics and Telecommunications (DET), University of Politecnico di Torino, Turin, Italy

ABSTRACT

Purpose and aim: Detection of brain tumors plays a critical role in the treatment of patients. Before any treatment, tumor segmentation is crucial to protect healthy tissues during treatment and to destroy tumor cells. Tumor segmentation involves the detection, precise identification, and separation of tumor tissues. In this paper, we provide a deep learning method for the segmentation of brain tumors.

Material and methods: In this article, we used a convolutional neural network (CNN) to segment tumors in seven types of brain disease consisting of Glioma, Meningioma, Alzheimer's, Alzheimer's plus, Pick, Sarcoma, and Huntington. First, we used the feature-reduction-based method robust principal component analysis to find tumor location and spot in a dataset of Harvard Medical School. Then we present an architecture of the CNN method to detect brain tumors.

Results: Results are depicted based on the probability of tumor location in magnetic resonance images. Results show that the presented method provides high accuracy (96%), sensitivity (99.9%), and dice index (91%) regarding other investigations.

Conclusion: The provided unsupervised method for tumor clustering and proposed supervised architecture can be potential methods for medical uses.

ARTICLE HISTORY
Received 29 May 2020
Revised 15 October 2020
Accepted 16 November 2020

KEYWORDS
CNN; MRI; brain tumor; robust PCA; segmentation

1. Introduction

Cancer can be defined as the uncontrolled growth and division of body cells. This leads to abnormal cell development and separation in the tissue of the brain as a tumor. This event is called a brain tumor. A brain tumor is an irregular brain injury that may be cancerous (malignant) or non-cancerous (benign). Although brain tumors are not very common, they are one of the deadliest types of cancers. Preliminary brain tumor detection plays a significant part in the likelihood of recovery and therapy. Techniques of medical imagery, such as computed tomography (CT) imaging, positron emission tomography, and single-photon emission CT, magnetic resonance spectroscopy, and magnetic resonance imaging (MRI) offers useful information on the brain tumors' form, length, site, and metabolism that enables detect brain tumors as quickly as possible. Although these techniques are employed in collaboration to include the most accurate brain tumor information, MRI is considered a well-known imaging method due to its good contrast in soft tissue as well as its wide availability. Before any treatment, tumor segmentation is critical to protect healthy tissues during treatment and to destroy tumor cells. Tumor segmentation involves the detection, precise identification, and separation of tumor tissues. This means that image segmentation involves manually interpreting by a human expert and segmenting a large number of multi-state MRI images. Many kinds of research have proposed computational methods for tumor detection and segmentation since segmentation is a time-consuming process and manual segmentation has a possibility of error. High performance in segmentation using deep learning methods has made these methods a good option for achieving this goal.

There are three approaches to image segmentation including pixel sorting, tracking boundaries of change, and the use of similarity and symmetry. The first method assumes that the pixels in each subclass have approximately fixed intensities which are usable for structures with similar physiological properties. These algorithms may identify multiple components at the same time, but they are weak in noise and inadequacy

CONTACT Mohsen Ahmadi mohsen.ahmadi@ine.uut.ac.ir Department of Industrial Engineering, Urmia University of Technology, Urmia, Iran.

in pictures. Conversely, methods that track the boundaries of change use intensity and spatial information. Therefore, a subclass must be uniform and enclosed within a boundary of change. The third method is to use border similarity and symmetry using local histograms. Diverse machine learning classification, segmentation, and clustering have been used in literature during the last years. Due to the high ability of feature extraction of big dataset pictures and 'no human interference', deep learning followed by the convolutional neural network (CNN) has got considerable attention in recent years. CNN based on deep learning concepts have more convolutional and hidden layers and is more powerful in the segmentation of pictures in comparison to conventional neural networks.

In this article, we address a CNN architecture for the segmentation of brain tumors for the seven brain diseases. First, the ground truth images are extracted from original images using robust principle component analysis (PCA). The results of segmentation performance analysis are presented in the following section.

2. Related works

The deep learning method is one of the interesting approaches between scholars. It has been employed in images, voice recognition, and identification of genotype/phenotype and classifying of diseases, such as target detection and segmentation. CNN is one of the well-known methods is classification and segmentation. CNN-based segmentation has been applied in many fields with a wide variety of applications ranging from image retrieval to object recognition such as conditional random fields in pattern and image recognition [1], objective detection, segmentation and localization [2], and medical applications such as CT images [3], breast tumors classification and detection [4], X-Ray image segmentation [5], Prostate segmentation from MRI [6], and widely used in brain tumors detection and segmentation from divers analysis images [7–9]. Among these utilities, CNN-based segmentation of MRI images to detect brain tumors has been investigated increasingly by researches for over past decade.

Chen et al. [10] suggested CNN architecture to fix some of the problems of image segmentation, such as indistinguishable features learned from standard convolution layers, where variations between components in terms of intensity, position, form, and size are subtle. They synthesized an architecture named Dense-Res-Inception Net to solve this problem. Their key modification was in three blocks named dense connection, residual inception, and unpooling blocks which leads a deeper and wider network.

Milletari et al. [11] presented an approach based on Hough voting to execute segmentation by leveraging the abstraction capabilities of CNNs. Their architecture was used the CNN classification results and was carried out voting by taking advantage of the features produced by the deepest portion of the network. Without the need for post-processing, the key to their design was to use fewer training data and offer smooth segmentation contours. This method is pretty good for big datasets. The exploration of small kernels in the segmentation images may also decrease the number of weights in the network and improve the processing time consequently. This task has been done by Pereira et al. [12] they also used intensity normalization as a preprocessing step. These adjustments managed to make MRI images effective for brain tumor segmentation. Hassantabar et al. [25] presented CNN architectures for classification and segmentation of X-Ray images of patients lung involved in the 2019 coronavirus. They used also a deep neural network with a fractal feature method for feature extraction of the images. Their method outperformed other approaches in the diagnosis and detection field (Table 1).

3. The method and materials

3.1. Proposed method

In this article, we detect brain tumor location using deep learning methods. The first step is the extraction of ground truth images from main images of seven types of brain lesions. In this step, we presented a new type of clustering method as Robust PCA for the extraction of tumor spots from other parts of images. After clustering images, we used enhancement methods to remove little spots from images. Then, the main images are allocated as the input layer of the CNN and ground truth images as the output layer. The training process is performed and consequently, results are recorded. The block diagram of the presented process is illustrated in Figure 1.

3.2. Robust principal component analysis (robust PCA)

One of the most important findings of linear algebra is the analysis of principal components since the simple and non-parametric approach is to derive meaningful details from confusing sets. In the PCA, data are depicted from a high-dimensional space to a low dimension, and in fact, the PCA is one of the methods

Table 1. Recent works on the CNN- and GAN-based segmentation.

Author	Year	Key work	Type	Method	Ref.
Havaei et al.	2016	Applying two pathway architecture based on both local details and global context	Brain tumor	CNN	[13]
Shakeri et al.	2016	Operation a CNN-based model on a full-blown 2D image without any arrangement at testing time	Sub-cortical structures of the brain	CNN	[14]
Pan et al.	2015	To exploit the learning power of the deep learning machine, apply the grading output on the test data measured by the sensitivity and specificity	Brain tumor	CNN	[15]
Fritscher et al.	2016	Using a patch-based segmentation to improve the accuracy	Brain tumor	CNN	[3]
Nema et al.	2020	Using a RescueNet based on the residual and mirroring principles.	Brain tumor	GAN	[16]
Rezaei et al.	2019	Using a voxel-GAN approach to improve the issue of unbalanced data for the tumor segmentation	Brain tumor	GAN	[17]
Chen et al.	2019	Applying an end-to-end GAN-based model	Brain tumor	GAN	[18]
Rundo et al.	2020	Using diverse architecture such as SegNet, U-Net, and pix2pix to segmentation the MRI images for prostate cancer	Prostate cancer	CNN	[19]
Kamnitsas et al.	2017	Using an 11 layer 3D convolutional architecture and a dual pathway for multi-scale processing	Brain lesion	CNN	[20]
Isola et al.	2017	Changed the classic GAN as the generator and the convolutional patch GAN classifier as the discriminator with U-net-based architecture	Multi images	GAN	[21]
Badrinarayanan et al.	2017	A modified encoder-decoder architecture called SegNet has been suggested	Multi images	CNN	[22]
Xue et al.	2018	An updated GAN called SegAN with a completely convolutional neural network was suggested as the segmentor to produce segmentation label maps	Medial images	GAN	[23]

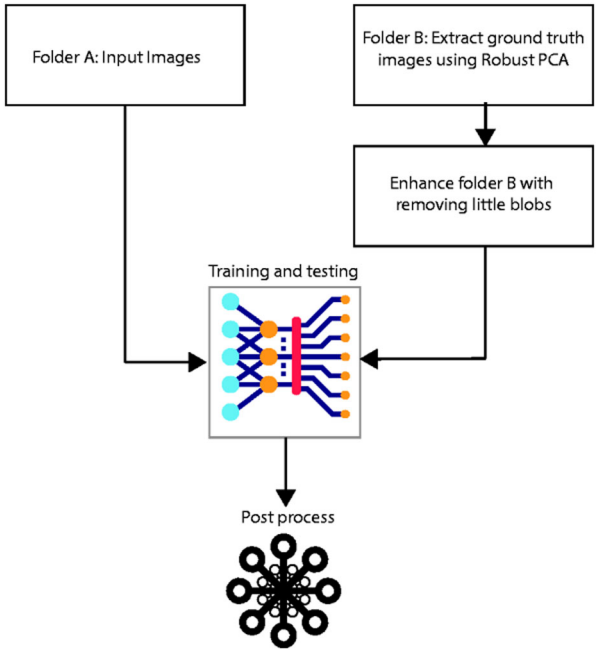

Figure 1. Conceptual diagram of the presented approach.

of selection of features and is required to decrease the dimension to explore the features in a simplified, lower-dimensional space. What PCA does is that it obtains a linear transformation that takes the vector of the h-dimensional properties to the d-dimensional properties of the vector (h < d), so that the information is kept almost completely (maximum possible information) and the least-squares mean error The PCA can be obtained by the minimization of the least-squares error, assuming that the vector of properties is $X \in R^d$ (d-dimensional space).

In Robust PCA for segmentation, the main process is abating of parameters L and S from the methods. These parameters are defined as follow:

$$L = D\left(\frac{1}{\mu}, X - S + \frac{Y}{\mu}\right) \tag{1}$$

$$S = S\left(\frac{\lambda}{\mu}, X - L + \frac{Y}{\mu}\right) \tag{2}$$

where X is input $m \times m$ image, μ is the augmented Lagrangian parameter, λ is the regularization parameter. The functions D is the shrinkage operator for singular values of the input image and S is shrinkage operator that defined follow:

$$D(\tau, X) = uv \times S(\tau, s) \tag{3}$$

$$S(\tau, X) = \frac{X}{|X|}\max(|X| - \tau,\ 0) \tag{4}$$

where u and v and s are the singular parameters of a symbolic matrix. The numeric unitary matrices consist of u as singular vectors, v diagonal matrix, and s singular values. Moreover, Y and Z are augmented Lagrangian multiplier is below:

$$Z = X - L - S \tag{5}$$

$$Y = \sum \mu Z \tag{6}$$

The iteration is repeated until E is reached to adequate value as follow:

$$E = \frac{|Z|}{|X|} < 10^{-5} \tag{7}$$

3.3. CNN

In this section, we explain the CNN deep learning approach. This type of neural network is one of the learning networks inspired by the Perceptron neural network. This deep network contains an input layer, an output layer, and a hidden deep layer. First, images or data of the problem are categorized into the algorithm and trained. Then the hidden output layer weights can appear in several ways [24]. If the output of the algorithm contains several numerical elements such as binary number or index then the proposed algorithm is a classification or detection algorithm. While, if the output layer is the matrix as large as the input image as ground truth images, the presented method is segmentation or detection. CNN consists of several hidden sublayer forms that are described as follows:

- **Convolutional layer**
  The center of the convolution network is the convolution layer, and its output can be represented as a three-dimensional neuron pile. In simple terms, a three-dimensional pile is the output of this sheet. The CNN network employs separate kernels in these layers to convolve the input image as well as the core function maps. There are three major advantages to the working of convolution [25]:
  - In each function map, the weight sharing process leads to a sharp decline in the number of parameters.
  - The local relation knows the correlation between the pixels of the neighbor.
  - A variation in the position of the object creates stability.
- **Activation functions**
  Commonly, activation mechanisms are implemented in the neural network to achieve the desired response from the input functions. For neural networks, various activation functions may be used; the sigmoid and hyperbolic tangent activation functions are the most relevant of them. Input that may have a value between $+\infty$ and $-\infty$ is obtained by the sigmoid function and the output is the interval between 0 and 1 [25]. An output value between 1 and -1 is given by the hyperbolic tangent function. This functionality makes these two features on CNN networks less widely used. Because multiple values are used in the matrix images, this outcome is the lack of image data and the device becomes unusable when using these functions in most situations (Figure 2) [25].

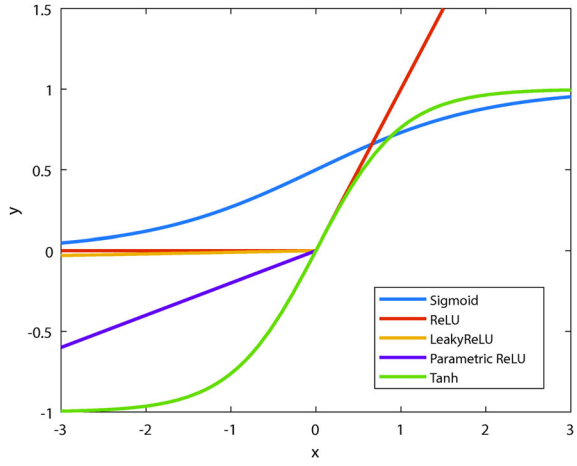

Figure 2. Plots of some types of activation functions.

- **Tan h function**
  The tan h function is similar to Sigmoid. The output interval of the tan h function is between -1 and 0 and, like Sigmoid, its curve is S-shaped. The advantage of tan h to Sigmoid is that in tan h, the negative input values are mapped to negative values, and the input value of zero is mapped to near zero. However, in sigmoid, negative values are written to values close to zero. The tan h function is also derivative and monotonically ascending.
- **ReLU**
  The rectified linear unit ReLU functionality is one of the activation functions introduced in recent years. ReLU is a function of activation that extends to all components. Its aim is to provide nonlinear behavior to the network. This functionality was implemented by Krizhevsky et al. in 2012. This function reaches all pixels in the image and renders all negative values zero, as can be seen in Formula 1. The aim of using ReLU is to describe a nonlinear component and its nonlinear training of the convolution neural network (Convolution is a linear method that is accomplished by the elements being multiplied and summed up) [25].
  This function is the most common activation function used in the CNN. The advantages of this function are:
- The gradient is not saturated in the positive region
- The calculations for the threshold requirements are simple.
- Works faster than sigmoidal and hyperbolic tangent function and reduces the training error rate
  Disadvantages of this function are:
- Outputs have no center of zero and values are always positive

- Gradients disappear for values smaller than zero, and new techniques such as RReLU, PReLU, and LeakyReLU are used to overcome this problem.
  Leaky ReLU For positive inputs it is the same as for the previous function, but for inputs smaller than zero it acts as $f(x) = 0.01x$. It reduces the negative numbers to very small (but effective) use. Its application is similar to the previous function. It is oblivious in the figure that the slope is shifted from $x = 0$ to the left, creating a leak and expanding the ReLU range.
- **SoftMax**
  One of the most used functions in the classification is the SoftMax function. In some cases, the SVM function is also used. But since the SoftMax function gives us a more accurate result of the probability of a class, it is, therefore, more suitable for classification. The probability of each class is calculated from the following formula.

$$P(y_i x_i; W) = \frac{e^{fy_i}}{\sum_j e^{f_j}} = \frac{Ce^{fy_i}}{C\sum_j e^{f_j}} = \frac{e^{fy_i} + \log C}{\sum_j e^{f_j} + \log C} \quad (8)$$

  Here y_i is the correct class for x_i image. Adding a constant coefficient such as C to both sides does not make a difference in the answer, but it makes the analysis easier. In this layer, a common value for this coefficient is assumed to be $\log C = -\max_j f_j$.
- **Dropout**
  Deep neural networks with a lot of parameters are powerful systems for learning. However, saturation occurs on some of these networks, which is the case on large networks that require a long time to train and test. Dropout is a technique that is currently widely used and is usually added as an extra layer after other layers. This layer works by randomly removing some units during network training. To do this task, consider a probability value of P, and the matrix is randomly generated as the input length. In this matrix, each value that has a probability more than the expected probability is kept and the other values are removed from the matrix. Dropout is a technique that prevents the network from being 'over-fit'. As its name implies, during the learning, some neurons are released by chance. This means that learning takes place on different architectures with different sets of neurons. Dropout can be considered as a group technique in which the outputs of multiple networks are blended to form the final output.
- **Max pooling**
  There are several effects of the use of max-pooling in neural networks. The use of max pooling enables the network, with only small adjustments to the image, to first define the object. Secondly, it helps the network to classify features with more image space. During the subtracting sampling task, pooling in the CNN is required to summarize the feature, so we can get into deeper network layers. The spatial information storage space reduces as a result of the sampling as we approach the end of each step and wish to reduce the sampling. So we want to begin pooling to gather what we have to retain this data. Max and average are the two most common ways of pooling [25].
  There is also much debate within the researches about how to improve each of the max and average techniques. The difference between the two is negligible, so one of the common paradigms is using max-pooling across the network to retain the best features and average pooling at the endpoints to get the final representation vector of the features before the last dense layer, and then deliver everything to SoftMax.
- **Padding**
  Sometimes the size of the output matrix needs to be controlled. An extra layer (with zero value) is added to all around the matrix in order to get an output matrix as same as the size of the input matrix. This job is called padding, same padding or 'zero paddings'. After applying the zero-padding and the filtration, the output image should have the same size as the original image.
- **Data augmentation**
  One of the most often overlooked issues is data preparation, preprocessing, and data enhancement. However, this task is not always necessary. Before running any kind of data processing, you must first check whether your task needs to be preprocessed.
  For example, in the classification of images, and implemented a standardized protocol for mean-normalization of images is based on the mean of the trained data. Researches have repeatedly shown that average normalization is the best thing to do for preprocessing. On the other hand, to optimize the images, mean-normalization can damage the network and produce less accurate results. Any task that is associated with very subtle differences in features such as color, appearance, the overall shape, and semantic differences in the image is likely to benefit from the lack of average normalization.
  Data Augmentation, on the other hand, is closely related to uniform performance enhancement both in absolute accuracy and in the generalization of the network. This is done in all types of tasks, such as high-level classification to low-level optimization. This means that the type of data augmentation used must be under consideration.

(a) (b) (c)

Figure 3. The results of the detection of tumor location: (a) original image, (b) the result of Robust PCA, (c) the result of image enhancement.

4. Results

4.1. Database

We used seven brain diseases in this article to introduce and validate the approaches proposed. They comprise of Glioma, Huntington, Meningioma, Select, and Sarcoma, Alzheimer's, Alzheimer's with visual agnosia. 80 MRI images from the Harvard Medical School website [26] are included in the image. In the axial plane, all images come from T2-weighted MR brain images and have 256×256 pixels. The photos are in a three-channel GIF format.

4.2. Preprocessing

Before starting the CNN segmentation process, some preprocesses are required. The input data is packages of images with GIF format; therefore, the first step is converting the dataset to RGB and then grayscale images. These steps transform three-channel images into single-channel images. The input images are mixtures of seven types of brain disease; therefore, the presented CNN method can be adopted to seven different types of brain MRI images. Second, preprocessing is the achievement of ground truth images. The ground truth images are the matrixes that determine the tumor location in binary format. Such that, the elements of matrixes in the location of tumor results 1 and other points equal 0. The ground truth images are determined in different ways, such as manual selection by physicians or using some images processing mathematical algorithms.

In this article, we used the Robust PCA method to reach the best ground truth images. Although the Robust PCA typically is used for feature reduction or determining outliers and special leverages, we used this method for detection of brain location in MRI images. This method used single-channel images for clustering the pixels of the image to two separate classes. With the use of Robust PCA, we reached to ground truth images. The results of this clustering algorithm are shown in Figure 3(b).

Figure 3 shows the results of determining ground truth images. To enhance the exact and clear location of the tumor, we extract only blobs larger than 150 pixels and removed the white small blobs. The resulting image is an acceptable ground truth image (Figure 3(c)). This two-step method determined the segmented images very quickly and was used for the seven types of brain disease with different μ and λ values. For training images using CNN, we need a huge amount of data to reached accurate results. Moreover, preventing from overfitting we need data augmentation. For the increasing number of images transform original images. We used the Gaussian function for adding noises, histogram equalization to enhance image contrasts, median filter, rotation in 90 degrees. We used these methods to produce input images. After augmentation of the original image, we have 1120 input and 1120 ground truth images.

4.3. Implementation of CNN architecture

To begin with, we present a deep architecture for a CNN. Three convolutional layers are used in this architecture. The diagram of the CNN layers is presented in Figure 4.

In this article, 1120 images were used for training the CNN architecture, and 80 images were used for testing the resulted weights. The first layer is a convolutional layer with the use of 32 filters in size of 3×3 with stride 1 in each direction. Also, the ReLU activation function is used for removing negative results.

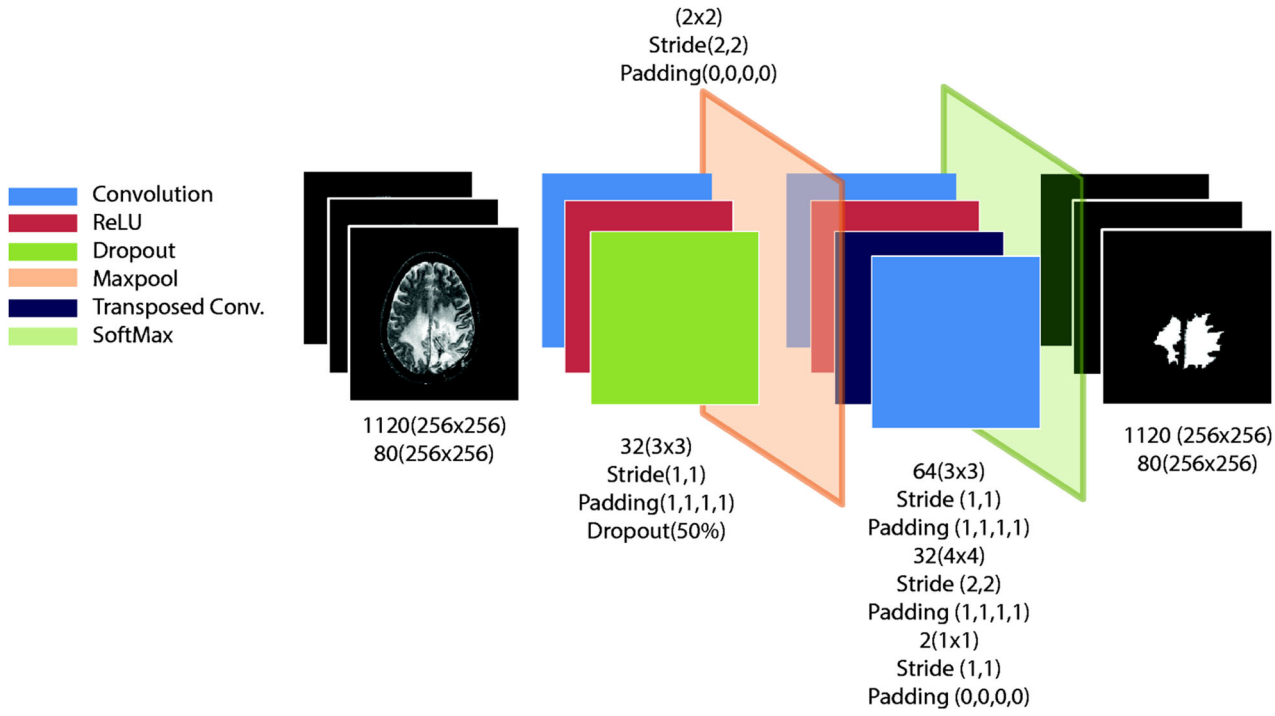

Figure 4. The architecture of presented CNN layers.

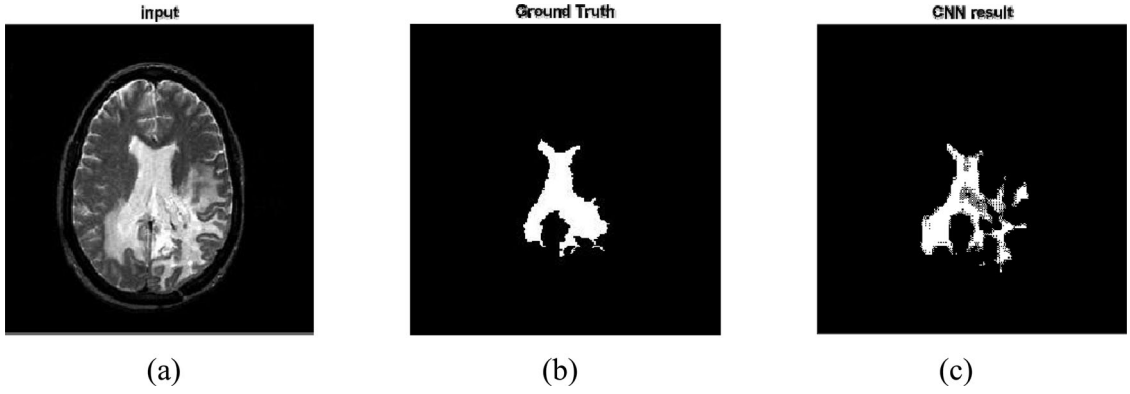

Figure 5. (a) Original image, (b) ground truth image, (c) CNN segmentation result.

Then use a dropout of 50%for dropping some items. The next layer is the Maxpooling function in 2×2 matrixes with stride 2 in each direction. The second convolutional layer consists of 64 (3×3) filters and a transposed convolutional layer is brought with 32 (4×4) filters. The final convolutional layer used two (1×1) filters to increase accuracy. The final step in the segmentation layers is SoftMax. Segmentation of images almost is the classification of pixels with ground truth images labels. The training process is performed with a training rate of 0.01 with 500 epochs. The resulted images are shown in Figure 5. The process is done for seven different brain diseases. Because of the better description of the results in regions with accumulated pixels, the probability of detection is higher than other pixels. Therefore, we calculate the probability of detection in each pixel. The resulted images for seven brain diseases are presented in Figure 6. The left contour shows the probability of tumor on images. So, the prediction presents reliable results.

5. Discussion

5.1. Performance analysis

In order to determine the outcome of binary classification (duality) of pixels, sensitivity, and specificity in the statistics of the two metrics are considered. The consistency of the outcomes of a test that

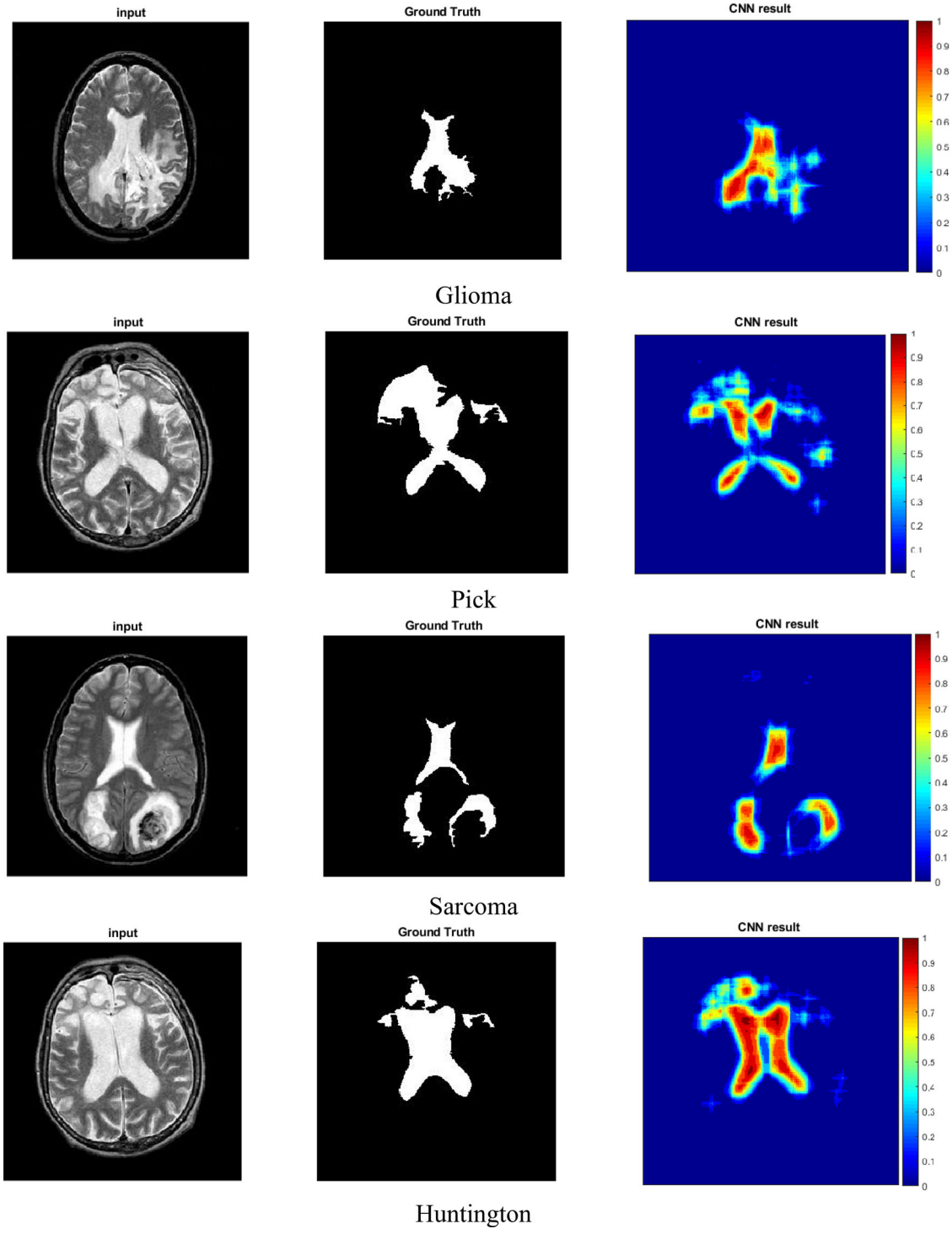

Figure 6. Results of segmentation using CNN, left: original images, middle: ground truth by robust PCA, right: CNN results.

separates the information into these two types is observable and informative using sensitivity and attribute metrics where the results can be separated into positive and negative classes. Sensitivity means the number of positive cases that would be accurately checked as positive. Specificity means the number of negative cases that accurately label them as negative [27].

- True positive (TP): The white pixel has been accurately detected.
- False positive (FP): The black pixel is detected inaccuracy.
- True negative (TN): The black pixel is detected accurately.
- False negative (FN): The white pixel is detected inaccuracy

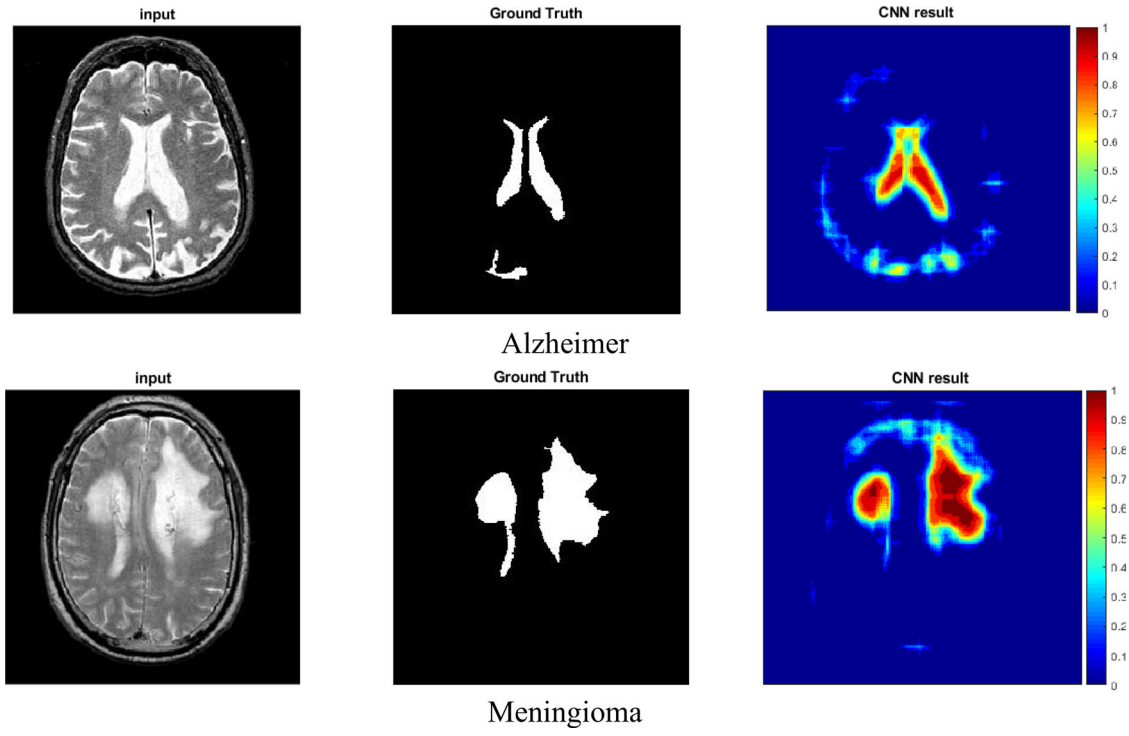

Figure 6. Continued

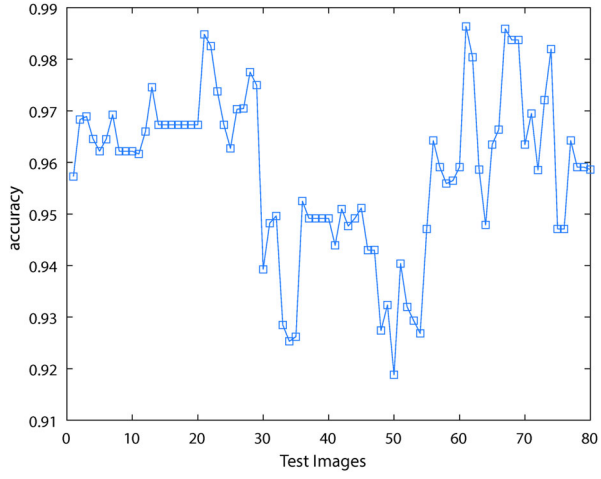

Figure 7. Accuracy of the test dataset.

The sensitivity of separating the percentages of TP cases into the sum of TP and FN cases in mathematical terms.

$$\text{Sensitivity,} \quad \text{TPR} = \frac{\text{TP}}{\text{TP} + \text{FN}} \tag{9}$$

Likewise, the specificity leads in the classification into the number of FP and TN cases of TN cases.

$$\text{Specificity, TNR} = \frac{\text{TN}}{\text{TN} + \text{FP}} \tag{10}$$

The sensitivity of the test and its specificity depend on the quality of the test and the type of test employed. Nevertheless, it is not possible to interpret the outcome of a test utilizing sensitivity and specificity alone.

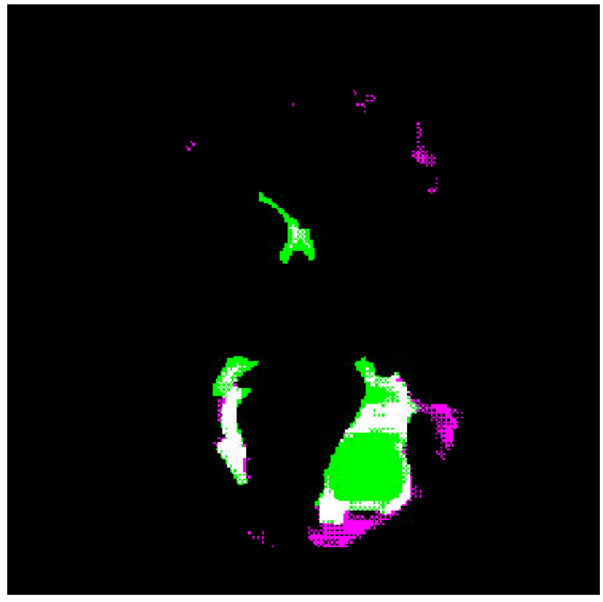

Figure 8. Pairwise images of GT and CNN.

$$\text{Precision,} \quad \text{PPV} = \frac{\text{TP}}{\text{TP} + \text{FP}} \tag{11}$$

$$\text{Accuracy (ACC)} = \frac{\text{TP} + \text{TN}}{\text{TP} + \text{TN} + \text{FP} + \text{FN}} \tag{12}$$

$$\text{Fall} - \text{out (FPR)} = \frac{\text{FP}}{\text{FP} + \text{FN}} \tag{13}$$

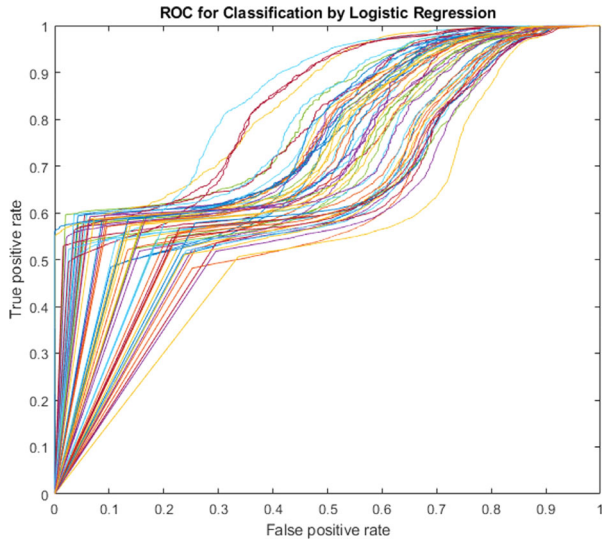

Figure 9. ROC curve for the presented approach.

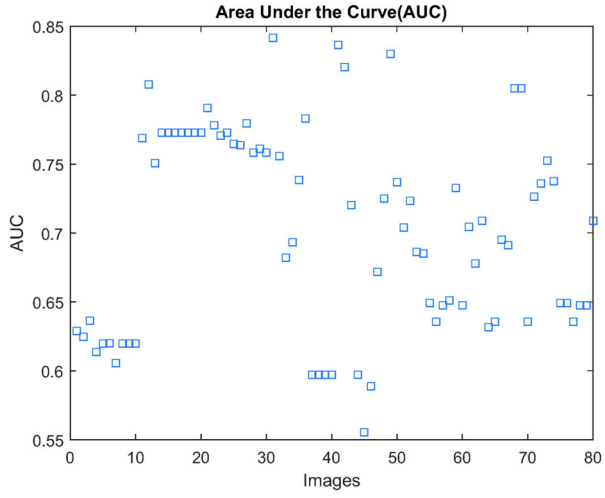

Figure 10. The area under the ROC curve (AUC) for the presented approach.

$$\text{Missrate} = \frac{\text{FN}}{\text{TP} + \text{FN}} \tag{14}$$

$$J = \frac{\text{TN}}{\text{TN} + \text{FP} + \text{FN}} \tag{15}$$

$$\text{Dice} = \frac{2J}{1 + J} \tag{16}$$

The ACC of the test images are shown in Figure 7. ACC is tolerated from 92% to 99%. The higher ACC corresponds to 0–30 or Alzheimer's, Alzheimer's plus, and Glioma almost 97%. Moreover, ACC of 60–80 has high accuracy. These diseases are detected with high accuracy. However, the ACC of 30–60 is corresponded to Huntington, Meningioma, and pick. The pairwise image of one case is depicted in Figure 8.

In Figure 8, one of the images of Sarcoma is presented. In this figure, the green spots show the intersection of GT and CNN and white color pixels are the points that exist in the GT but not predicted properly. In other words, green pixels show the TP and white pixels show the FN pixels. Also, Purple points are the paints that are predicted as a tumor spot incorrectly, which is names FP. Other back points show the TN. Figure 9 shows the ROC curve of images used in this article for segmentation using the CNN method. This chart shows the TP rate versus the FP rate. Regarding results, if the curve inclines to TP rate = 1 and FP rate = 0, the presented method reveals high performance. Each of the curves is belonging to an image. Usually, the ROC curve for better description is illustrated as under the curve area or AUC. For every image with a high AUC value, the presented method results in high performance. The AUC values are depicted on the chart in Figure 10. Based on the findings of Figure 10, the AUC value for all of the images is averaged to 0.7031 which is an acceptable value for the CNN method.

Total performance analysis values are summarized as following Table 2. Regarding these findings total accuracy is 96% that shows the high performance of this method. The values of specificity, sensitivity, and dice index are 99.8%, 99.9%, and 91.2%, respectively.

Table 3 shows the comparison of the presented method using the Dice index. Results show that the presented method shows a high dice index and acceptable architecture.

Table 2. The average of performance criteria values for the CNN method.

Criteria	AUC	Fallout	Miss rate	Dice	Sensitivity	Specificity	Accuracy
Mean Value	0.70	0.002	0.001	0.912	0.999	0.998	0.96

Table 3. The comparison of the presented architecture with other methods.

Reference	Method of Detection	Ground truth	Dice index
[28]	Experimental	Manual	0.88
[29]	SVM	Semi-automatic	0.86
[30]	CNN	K-means	0.83
[31]	GAN	Automatic	0.8
[16]	Unpaired GAN	Automatic	0.94
[12]	CNN	Automatic	0.78
[32]	2D cGAN	Automatic	0.59
[32]	32 cGAN	Automatic	0.72
Presented method	CNN	Robust PCA	0.91

6. Conclusion

Automated detection of brain disease plays a critical role in the treatment of patients. So, investigations in the fields of medical image processing are the next

step in medical technology. In this article, we presented two approaches to the detection of seven types of brain lesions. The first method is the Robust PCA. This method was used as clustering data and feature reduction in recent researches. We used this property of robust PCA to separate lesion area from brain MRI images. The Robust PCA cluster input images to two separate black and white clusters. This clustering process almost can detect tumor location. Therefore, the other small hit points are enhanced with the use of algorithms that remove small spots. The resulting images are used as ground truth images to the next step. The second methods are a CNN. We used result images of robust PCA in the CNN algorithm. The input layer of the CNN method is a folder of gray MRI images with a size of 256×256. On the other hand, the output layer is consisting of the ground truth images. For the increasing number of images and preventing from overfitting, we used the data augmentation approach. With the use of rotation, noise, and filtration the numbers of images are increased to 2240 images. Results are depicted based on the probability of tumor location in MRI images. The higher ACC corresponds to 0-30 or Alzheimer's, Alzheimer's plus, and Glioma almost 97%. Moreover, ACC of 60–80 has high accuracy. These diseases are detected with high accuracy. However, the ACC of 30–60 is corresponded to Huntington, Meningioma, and pick. Results show that the presented method provides higher accuracy (96%), sensitivity (99.9%), and dice index (91%) than other researches.

Disclosure statement

No potential conflict of interest was reported by the author(s).

Funding

The funding sources had no involvement in the study design, collection, analysis or interpretation of data, writing of the manuscript, or in the decision to submit the manuscript for publication.

ORCID

Mohsen Ahmadi http://orcid.org/0000-0003-1550-110X
Abbas Sharifi http://orcid.org/0000-0002-2915-2740

References

[1] Liu F, Lin G, Shen C. CRF learning with CNN features for image segmentation. Pattern Recognit. 2015; 48(10):2983–2992.

[2] Cai Z, Vasconcelos N. Cascade R-CNN: High-Quality Object Detection and Instance Segmentation. arXiv preprint arXiv:1906.09756, 2019.

[3] Fritscher K, Raudaschl P, Zaffino P, et al. Deep neural networks for fast segmentation of 3D medical images. In: International Conference on Medical Image Computing and Computer-Assisted Intervention, 2016. p. 158–165.

[4] Rouhi R, Jafari M, Kasaei S, et al. Benign and malignant breast tumors classification based on region growing and CNN segmentation. Expert Syst Appl. 2015;42(3):990–1002.

[5] Bullock J, Cuesta-Lázaro C, and Quera-Bofarull A. XNet: a convolutional neural network (CNN) implementation for medical x-ray image segmentation suitable for small datasets. In: Medical Imaging 2019: Biomedical Applications in Molecular, Structural, and Functional Imaging, 2019. p. 109531Z.

[6] Zhu Q, Du B, Turkbey B, et al. Deeply-supervised CNN for prostate segmentation. In: 2017 International Joint Conference on Neural Networks (IJCNN), 2017, p. 178–184.

[7] Milletari F, Navab N, and Ahmadi S-A. V-net: Fully convolutional neural networks for volumetric medical image segmentation. In: 2016 Fourth International Conference on 3D Vision (3DV), 2016. p. 565–571.

[8] Kayalibay B, Jensen G, Smagt PVD. CNN-based segmentation of medical imaging data. arXiv preprint arXiv:1701.03056, 2017.

[9] Moeskops P, Wolterink JM, van der Velden BHM, et al. Deep learning for multi-task medical image segmentation in multiple modalities. In: International Conference on Medical Image Computing and Computer-Assisted Intervention, 2016. p. 478–486.

[10] Chen L, Bentley P, Mori K, et al. Drinet for medical image segmentation. IEEE Trans Med Imaging. 2018; 37(11):2453–2462.

[11] Milletari F, Ahmadi S-A, Kroll C, et al. Hough-CNN: deep learning for segmentation of deep brain regions in MRI and ultrasound. Comput Vis Image Underst. 2017;164:92–102.

[12] Pereira S, Pinto A, Alves V, et al. Brain tumor segmentation using convolutional neural networks in MRI images. IEEE Trans Med Imaging. 2016;35(5):1240–1251.

[13] Havaei M, Davy A, Warde-Farley D, et al. Brain tumor segmentation with deep neural networks. Med Image Anal. 2017;35:18–31.

[14] Shakeri M, Tsogkas S, Ferrante E, et al. Sub-cortical brain structure segmentation using F-CNN's. In 2016 IEEE 13th International Symposium on Biomedical Imaging (ISBI), 2016. p. 269–272.

[15] Pan Y, Huang W, Lin Z, et al. Brain tumor grading based on neural networks and convolutional neural networks. In 2015 37th Annual International Conference of the IEEE Engineering in Medicine and Biology Society (EMBC), 2015. p. 699–702.

[16] Nema S, Dudhane A, Murala S, et al. RescueNet: an unpaired GAN for brain tumor segmentation. Biomed Signal Process Control. 2020;55:101641.

[17] Rezaei M, Yang H, and Meinel C. voxel-GAN: Adversarial Framework for Learning Imbalanced Brain Tumor Segmentation: 4th International Workshop,

BrainLes 2018, Held in Conjunction voxel-GAN: Adversarial Framework for Learning Imbalanced Brain Tumor Segmentation, 2019.

[18] Chen H. Brain tumor segmentation with generative adversarial nets. 2019 2nd International Conference on Artificial Intelligence and Big Data (ICAIBD), 2019. p. 301–305.

[19] Rundo L, Han C, Zhang J, et al. CNN-based prostate zonal segmentation on T2-weighted MR images: a cross-dataset study. In Neural approaches to dynamics of signal exchanges. Springer; 2020. p. 269–280.

[20] Kamnitsas K, Ledig C, Newcombe VF, et al. Efficient multi-scale 3D CNN with fully connected CRF for accurate brain lesion segmentation. Med Image Anal. 2017;36:61–78.

[21] Isola P, Zhu J-Y, Zhou T, et al. Image-to-image translation with conditional adversarial networks. In Proceedings of the IEEE Conference on Computer Vision and Pattern Recognition, 2017. p. 1125–1134.

[22] Badrinarayanan V, Kendall A, Cipolla R. Segnet: A deep convolutional encoder-decoder architecture for image segmentation. IEEE Trans Pattern Anal Mach Intell. 2017;39(12):2481–2495.

[23] Xue Y, Xu T, Zhang H, et al. Segan: Adversarial network with multi-scale L1 loss for medical image segmentation. Neuroinformatics. 2018;16(3-4):383–392.

[24] Krizhevsky A, Sutskever I, Hinton GE. Imagenet classification with deep convolutional neural networks. In Advances in Neural Information Processing Systems. 2012. p. 1097–1105.

[25] Hassantabar S, Ahmadi M, Sharifi A. Diagnosis and detection of infected tissue of COVID-19 patients based on lung x-ray image using convolutional neural network approaches. Chaos Solitons Fractals. 2020; 140(140):110170.

[26] The Whole Brain Atlas. http://www.med.harvard.edu/AANLIB/.

[27] Hamzenejad A, Jafarzadeh Ghoushchi S, Baradaran V, et al. A robust algorithm for classification and diagnosis of brain disease using local linear approximation and generalized autoregressive conditional heteroscedasticity model. Mathematics. 2020;8(8):1268.

[28] Menze BH, Jakab A, Bauer S, et al. The multimodal brain tumor image segmentation benchmark (BRATS). IEEE Trans Med Imaging. 2015;34(10):1993–2024.

[29] Havaei M, Larochelle H, Poulin P, et al. Within-brain classification for brain tumor segmentation. Int J Comput Assist Radiol Surg. 2016;11(5):777–788.

[30] Dvorak P, Menze B. Structured prediction with convolutional neural networks for multimodal brain tumor segmentation. In: Proceedings of the Multimodal Brain Tumor Image Segmentation Challenge; 2015. p. 13–24.

[31] Rezaei M, Harmuth K, Gierke W, et al. A conditional adversarial network for semantic segmentation of brain tumor. In International MICCAI Brainlesion Workshop; 2017. p. 241–252.

[32] Yu B, Zhou L, Wang L, et al. 3D cGAN based cross-modality MR image synthesis for brain tumor segmentation. In 2018 IEEE 15th International Symposium on Biomedical Imaging (ISBI); 2018. p. 626–630.

[33] Sun Y, Zhou C, Fu Y, et al. Parasitic GAN for semi-supervised brain tumor segmentation. In 2019 IEEE International Conference on Image Processing (ICIP), 2019. p. 1535–1539.

[34] Dong X, Lei Y, Wang T, et al. Automatic multiorgan segmentation in thorax CT images using U-net-GAN . Med Phys. 2019;46(5):2157–2168.

[35] Han C, Rundo L, Araki R, et al. Infinite Brain Tumor Images: Can GAN-based Data Augmentation Improve Tumor Detection on MR Images? In Proceeding Meeting on Image Recognition and Understanding (MIRU), 2018.